Available online at www.sciencedirect.com
ScienceDirect
International Journal of Multiphase Flow 33 (2007) 789–796
International Journal of Multiphase Flow
www.elsevier.com/locate/ijmulflow

Brief communication

Direct numerical simulations of two-layer viscosity-stratified flow, by Qing Cao, Kausik Sarkar, Ajay K. Prasad, Int. J. Multiphase Flow (2004) 30, 1485–1508

Theo G. Theofanous *, Robert R. Nourgaliev, Suthee Wiri

Center for Risk Studies and Safety, University of California, Santa Barbara, CA 93106, USA

Received 15 June 2006; received in revised form 3 February 2007

The purpose of this Communication is to call into question the Cao, Sarkar, and Prasad (2004, CSP) conclusions about the validity of the diffuse interface method for direct numerical simulations of such (shear) flows. This has also an impact on understanding the interfacial-instability physics of sharp vs. diffuse (smeared, sheared) interfaces.

We discovered the issue in trying to understand the CSP code-benchmark comparisons with our DNS code MuSiC-SIM (Nourgaliev et al., 2006a,b,) – the "SIM" stands for "Sharp Interface Method". Our code solves the Navier–Stokes equations in a multi-fluid system by matching the flow fields across interfaces (as is the case for immiscible fluids) through the exact (jump) conditions. The code used by CSP is based on a widespread modeling idea that "imbeds" interfaces in the same overall calculation (of a single "fluid") as "smeared" or "diffuse" transition regions for fluid properties (density, viscosity, etc.), hence, "Immersed Boundary Method", or "Diffuse Interface Method" (DIM) – see for example Griffith and Peskin (2005). The other key ingredient of this modeling approach is that the surface tension is modeled as a volume source in the momentum equation, again smeared over the "thin" transition regions (the "Continuous Surface Force" approach) – Brackbill et al. (1992), Unverdi and Tryggvason (1992).

In making our points here we bring to bear also linear stability analyses as implemented in our computer code AROS (All-Regime Orr–Sommerfeld). The AROS code involves domain-decomposition and Chebyshev Collocation Methods applied to the linearized Navier–Stokes equations (the Orr–Sommerfeld formulation). We use high-order Chebyshev polynomials and quadruple precision to permit convergent eigensystem analysis (even for large density/viscosity ratios) with the QZ algorithm. The code has been extensively verified as summarized in Table 1, and in turn it has been used as the standard for verification of MuSiC-SIM in the linear regime. Subsequently, it has also been used for the study of the effects of smearing (physical, or numerical) on linear stability of interfaces in shear-dominated flows.

We shall show that (a) the validation tests performed by CSP (their Section 4.1.2) are in fact less compelling than suggested by their results; in particular the linear stability results published by others that they used for comparison are in error, and (b) the results presented to support their non-linear stability discussion (their Section 4.2.1) are inaccurate. Further, we shall present results to make it evident that these errors are not the fault of CSP but they are inherent in all DIM methods, which are in fact not suitable for DNS of shear-dominated flows.

* Corresponding author. Tel.: +1 805 893 4900; fax: +1 805 893 4927.
E-mail address: theo@theo.ucsb.edu (T.G. Theofanous).

0301-9322/$ - see front matter
doi:10.1016/j.ijmultiphaseflow.2007.03.001

Table 1
Scope of the AROS-verification effort

Reference cited	Flow	Figure/Table-variable(s)
Orszag (1971)	Single-phase Poiseuille	Table 2[a] – eigenvalues
		Table 4[a] – R_{cr}
Yih (1967)	Sharp interface Couette, Poiseuille	Eq. (46)[a] – asymptotic eigenvalue (equation)
Yiantsios and Higgins (1988)	Sharp interface Couette, Poiseuille	Table 1[a] – eigenvalues(with *S*)
		Fig. 4/6[b] – *n* vs wavenumber (with *S*)
		Fig. 8[c] – eigenvalue vs wavenumber (with gravity)
		Fig. 11[c] – eigenvalue vs wavenumber
		Fig. 12a/b[b] – wavenumber vs *R*, *m* vs *Re*
Su and Khomami (1992)	Sharp interface Poiseuille	Table 1[a] – eigenvalues for wavenumber of 10^{-5}
		Table 2[a] – eigenvalues for wavenumber of 10^{-2}
		Fig. 2[b] – *n* vs wavenumber
Boeck and Zaleski (2005)	Sharp interface free shear mixing	Fig. 7[c] – Growth factor vs wavenumber
		Fig. 12[c] – Growth factor vs wavenumber (with *S*)
Pinarbasi and Liakopoulos (1995)	Diffuse interface Poiseuille	Fig. 5[c] – eigenvalue vs wavenumber
Coward et al. (1997)	Sharp interface Couette	Table I[a] – leading eigenvalues
		Table II[a] – eigenvalues
Malik and Hooper (2005)	Diffuse interface Poiseuille	Fig. 2[c] – eigenvalue distribution (single fluid)
		Fig. 3[c] – eigenvalue distribution (diffuse interface)
		Table 3[a] – eigenvalues

S – surface tension included.
[a] Agreement with numerical value.
[b] Agreement with neutral stability curves.
[c] Graphical agreement.

(a) *The code validation case of CSP* was made by comparing growth factors (K) obtained from numerical results of wave-amplitude-variation with time fit to

$$a^* = a_0^* e^{Kt^*} \tag{1}$$

with linear stability results from Khomami and Su (2000) (KS), as presented in CSP's Table 3. Eq. (1) is for a frame translating with the interfacial velocity U_0, and t^* is based on U_0 and the channel depth $d = d_1 + d_2$ of a two-fluid system. In dimensionless terms the results depend on the depth ratio $n = d_1/d_2$, viscosity ratio $m = \mu_1/\mu_2$ the wave-number $\alpha = 2\pi/\lambda$, and the flow Reynolds number $R = U_0 d_v \rho/\mu_v$ where subscript v denotes the more viscous of the density-matched fluids. In addition, CSP found that two dynamically similar cases (obtained by inverting the m and n) produced the same numerical results as exhibited in their Table 2. Specifications and results for all these cases are reproduced here in respective Tables 2 and 3 along with several additions and explanations as follows:

1. The KS linear stability results are inaccurate (by comparison to AROS and new calculations by Khomami) as seen in Figs. 1a,1b and Table 3. The KS error (a 25% under-prediction) has been documented in Theofanous et al. (in press).
2. In Figs. 1a, 1b and Table 3 we can see that CSP have found one excellent and one reasonably good agreement with the two erroneous KS results.

Table 2
Growth factors for the two pairs of dynamically similar cases of CSP (the CSP taken from their Table 2)

	Case 1	Case 2	Case 3	Case 4
	$R = 7.1$; $m = 2$; $n = 0.25$	$R = 7.1$; $m = 0.5$; $n=4$	$R = 5.4$; $m = 2$; $n = 0.33$	$R = 5.4$; $m = 0.5$; $n = 3$
CSP	0.216	0.216	0.210	0.209
AROS	0.282	0.282	0.207	0.207

Table 3
Growth factors for the two cases treated by KS (the CSP taken from their Table 3)[a]

	m	n	R[b]	α	KS	CSP[a]	AROS
Case 1	0.203	3.330	0.009	0.72	0.0014[c]	0.0014	0.0019
Case 2	0.203	4.875	0.007	0.53	0.0020	0.0016	0.0026

[a] For the purposes of this table CSP adopted the normalization used by KS rather than their own.
[b] These are the correct Reynolds numbers (Theofanous et al., in press).
[c] The correct value from KS is 0.0015 (this is why the CSP point in Fig. 1a is off the KS line).

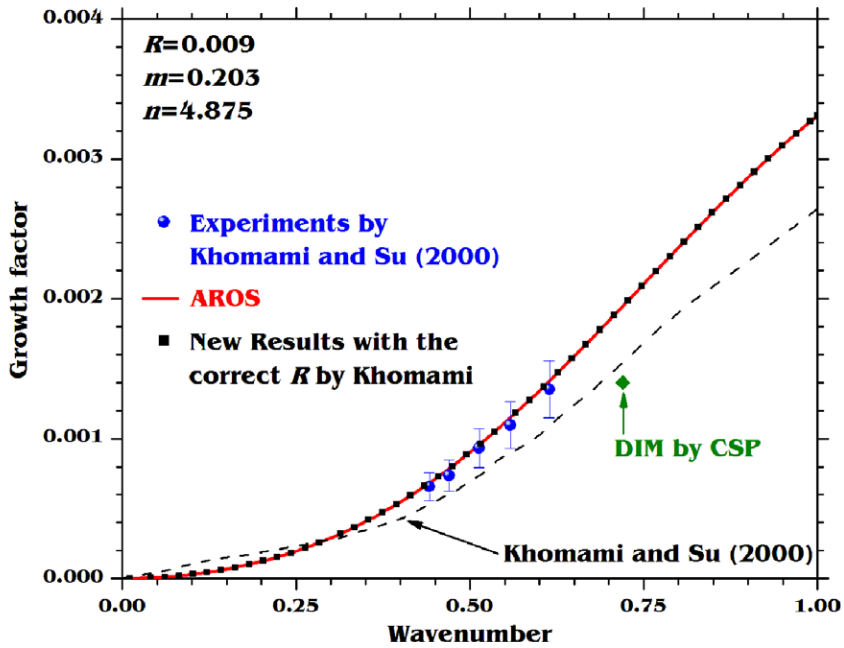

Fig. 1a. The growth factor found in Case 1 of CSP, and the Khomami and Su (2000) Orr–Sommerfeld curve from which Case 1 was defined, in comparison with AROS, new results by Khomami, and experiments by Khomami and Su (2000).

3. While the definition (the m, n and α values) of the two KS cases considered by CSP is correct, the R values in CSP Table 3 are incorrect (they appear to have been reversed) – we show the correct values and CSP have kindly confirmed that the error occurred in setting up their table. The CSP results can be seen to be off by 16% and 46%.
4. As Table 2 shows, of the two CSP consistency tests, the one is in excellent agreement while the other is off by 23% with respect to AROS.

(b) *A partial accounting of other problems with CSP in support of their non-linear simulations* will be made by reference to their Figs. 2 and 8. Fig. 2 is important because it was said to be typical of all their results. Fig. 8 is important because based on it CSP speculate about non-linear effects and transient growth, a subject of considerable current interest.

In regards to their Fig. 2, reproduced here as Fig. 2, along with our results from AROS, MuSiC-SIM, and MuSiC-DIM, the following can be noted:

1. The CSP result exhibits a significantly lower (by 30%) growth factor as compared to the accurate AROS (and MuSiC-SIM) results. The MuSiC-SIM simulations were found to require grids in excess of a few hundred nodes (per wavelength) to attain asymptotic grid convergence (see Table 4), and the result is in perfect agreement with AROS. This suggests that the reported convergence observed by CSP with their grids of

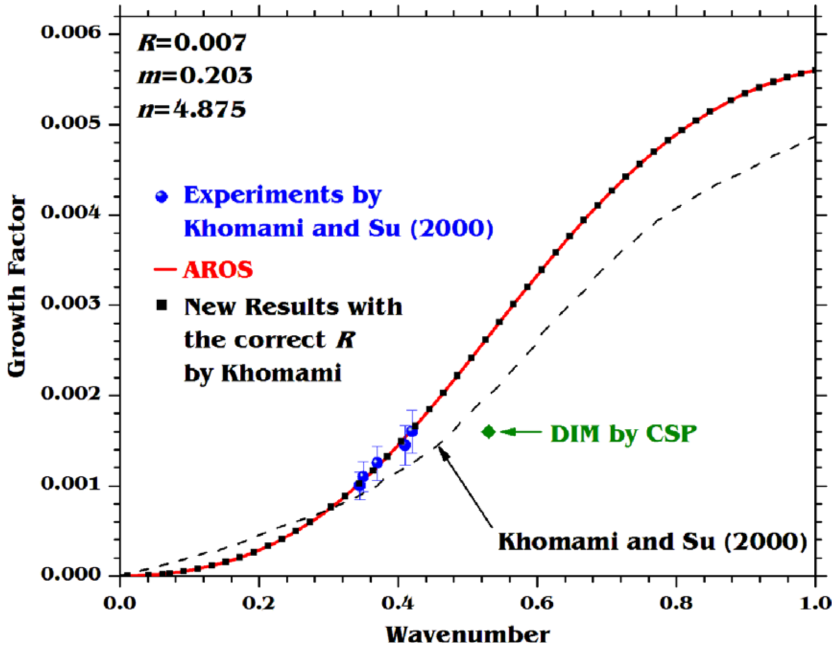

Fig. 1b. The growth factor found in Case 2 of CSP, and the Khomami and Su (2000) Orr–Sommerfeld curve from which Case 2 was defined, in comparison with AROS, new results by Khomami, and experiments by Khomami and Su (2000).

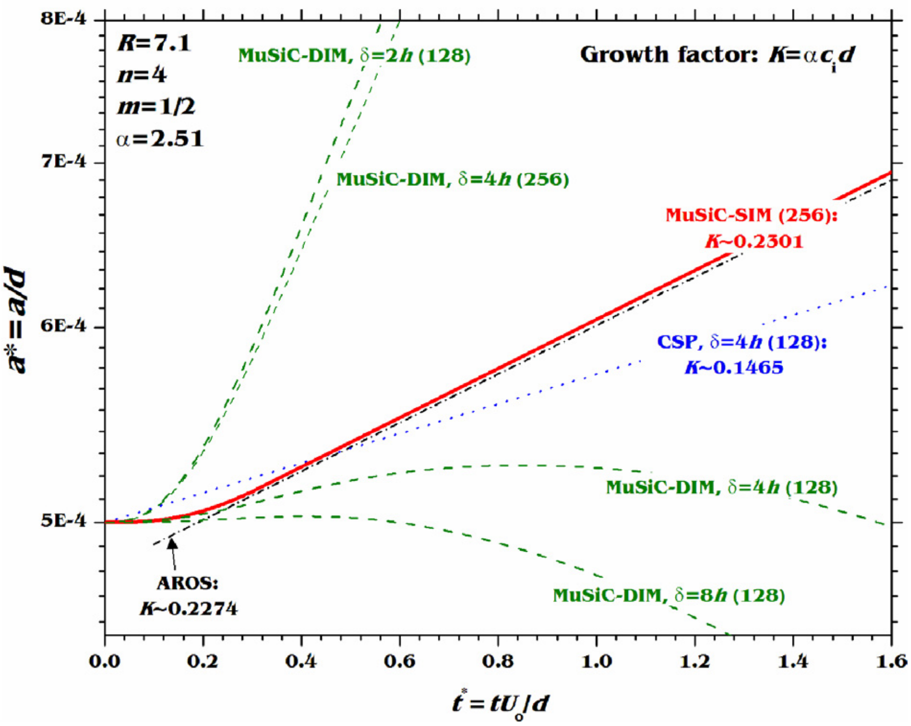

Fig. 2. A ‘‘typical’’ instability amplitude-growth found by CSP (taken from their Fig. 2), in comparison with the SIM and various DIM results by MuSiC. The numbers in parentheses represent the number of grids per wave-length (λ), h is the grid spacing, δ is the smear layer thickness, a is wave amplitude and d is the combined thickness of upper and lower fluids. A sine was used as the mollifying function in this sample of DIM simulations.

Table 4
Grid convergence study with SIM_3

Grid resolution	K^*	L_1-norm
$256/\lambda$	0.2481	0.0207
$512/\lambda$	0.2343	0.0069
Rate:		1.585[a]

$R = 7.1$, $m = 0.5$, $r = 1$, $S = 0$, $n = 4$, $\alpha = 2.5133$, $\varepsilon = 5 \times 10^{-4}$. The exact (AROS) K^* is 0.2274.

[a] The somewhat lower than the theoretical, 2nd-order convergence rate (for SIM_3) is from accuracy losses due to (a) piecewise-linear representation of the interface, and (b) numerical mappings between the structured-unstructured grids.

64×64 and 128×128 nodes (admittedly with a different code and therefore a different implementation of the DIM) was in fact due to a spurious (or at least inaccurate) solution. This could be due to the fact that their method is first-order accurate in velocity, and therefore zero-order accurate in shear stress as is the case with any DIM code (Nourgaliev et al., 2006a). Note that MuSiC-SIM is third-order accurate in both space and time.

2. In fact, as shown in Fig. 3, a 64×64 grid is not sufficient to resolve the critical layer – as the energy flows in the figure show, and as it is well known, instability growth depends critically on the proper resolution in the immediate neighborhood of this layer. Also from this figure one can see that a good simulation would require a 256×256 grid at a minimum, which is consistent with what we found in our simulations with MuSiC-SIM.
3. As shown by the MuSiC-DIM results in Fig. 2, the growth rate depends on the amount of smearing (number of cells over which the transition region is defined), and degree of discretization (number of grid points per wave-length) – these control indirectly the amount of "effective" discontinuity in viscosity at the interface, which is responsible for the instability. As expected, the operating parameter in this is the ratio of number of grid points used in smearing divided by the number of grids used per wave-length. When this ratio is large enough, even an unstable interface may appear stable (see the $8h[128]$ case in Fig. 2). With this hindsight one realizes that, since the result depends on the implementation details of each particular DIM method, even the correct result may be recovered by chance; however a rigorously convergent, and correct result is only accessible by a sharp treatment of the interface (MuSiC-SIM).

In regards to the CSP Fig. 8a, reproduced here as Fig. 4 ($R = 0.47$, $m = 0.5$, $n = 0.111$), along with results from AROS, the following comments are offered for consideration:

1. The (asymptotic) long-wave analysis (Yih, 1967; Yiantsios and Higgins, 1988) as applied by CSP predicts that all four wavelengths considered are linearly stable, while our linearized stability analysis (using AROS) shows that two of them are stable ($\lambda^* = 1$ and $\lambda^* = 0.5$) and the other two unstable ($\lambda^* = 0.125$ and $\lambda^* = 0.25$) – see Fig. 5. The reason for this apparent discrepancy is that the condition of applicability of the asymptotic result ($\alpha R < 1$) is not satisfied for any of the four wave-numbers considered by CSP in this exercise – see Table 5.
2. For the two stable cases, one of the CSP numerical results is reasonably close to the correct one (5%), the other is significantly off (42%).
3. For the two unstable cases, the CSP results exhibit unstable, pulsatile growth at rates that are distinctly off the correct results.
4. Commenting on the discrepancy between their long-wave theory prediction and their numerical results CSP note that: "The global trend is towards more unstable behavior for smaller λ^*... Hooper and Grimshaw (1985) attributed increasing amplitude to the non-linear convective term in evolution equation, and decreasing amplitude to energy transfer to higher harmonics ... it appears that other non-linear mechanisms exist in addition to the energy transfer between modes", and they conclude that:"Further studies are required to resolve this issue". Our results show that in fact there is no issue.

Conclusions: Thus we have to conclude that subject paper results fail to support the accuracy of DIM-based simulations in the linear instability regime for the two-layer, viscosity-stratified flow system considered.

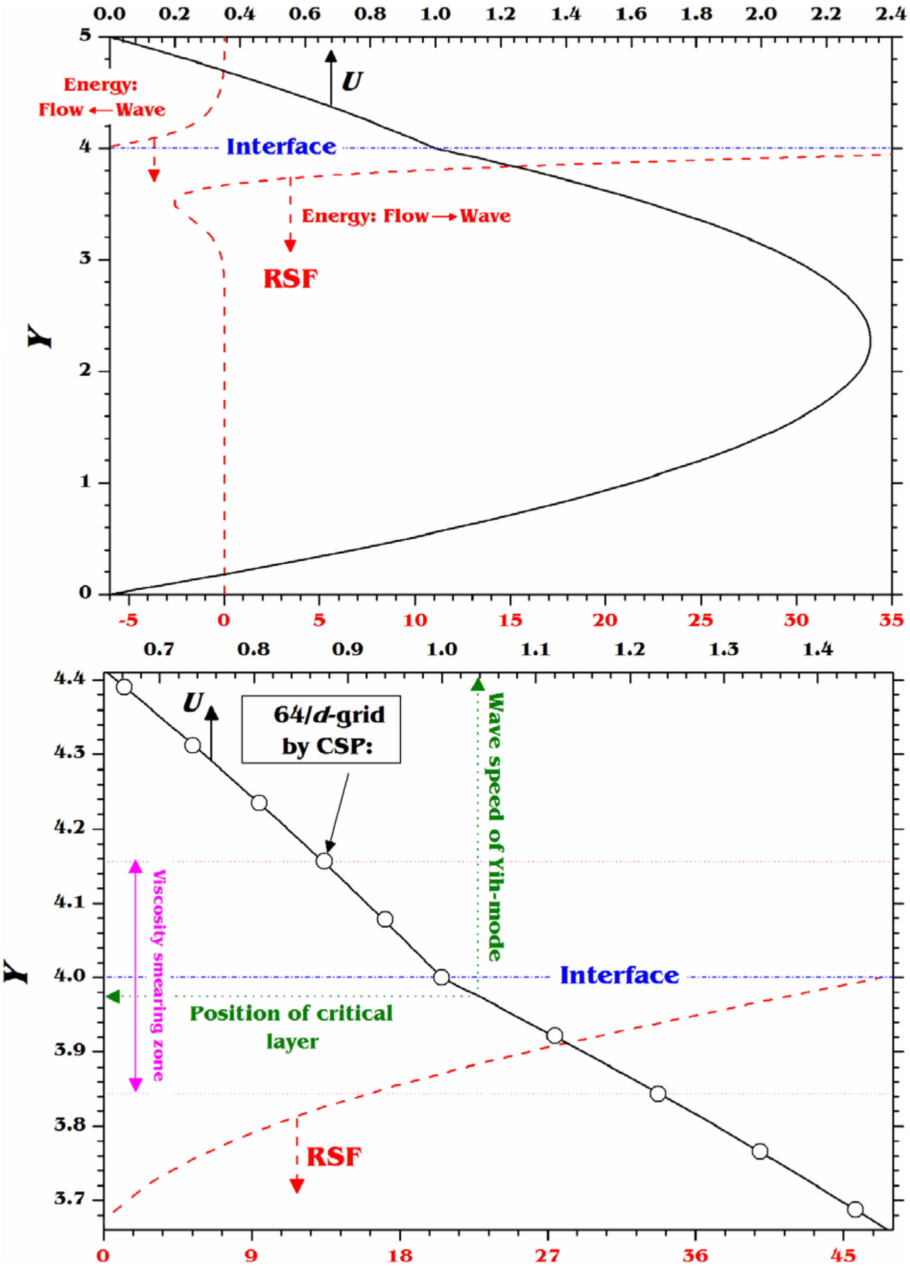

Fig. 3. (*Top*) Mean-flow velocity (U) and Reynolds-Stress-Function (RSF) profiles for the case found in CSP's Fig. 2, showing the energy flows that drive and dissipate the instability. (*Bottom*) A close-up view of the critical layer and "viscosity-smearing" regions. The RSF and wave-speed of the Yih-mode are directly obtained from AROS. RSF is computed as discussed in Malik and Hooper (2005). The critical layer position (y_{cr}) is found by the condition $U(y_{cr}) = C_R$, where C_R is the wave speed found from the eigenvalue problem (Drazin, 1962). It can be seen that the interfacial wave "extracts" its energy from the less viscous fluid (right below the interface, RSF > 0) and looses some of it to the more viscous fluid (above interface, RSF < 0). With a grid of 64/d as used by CSP, the critical layer is severely under-resolved.

Moreover based on the sample MuSiC-SIM, AROS, and MuSiC-DIM results provided here, along with additional evidence in Nourgaliev et al. (2006b), we suggest that any such attempt would be doomed to failure. We believe this is a general conclusion, albeit the particulars, such as the amounts of error incurred, would depend, in addition to the smearing parameters as noted above, on the type of mollifying function used.

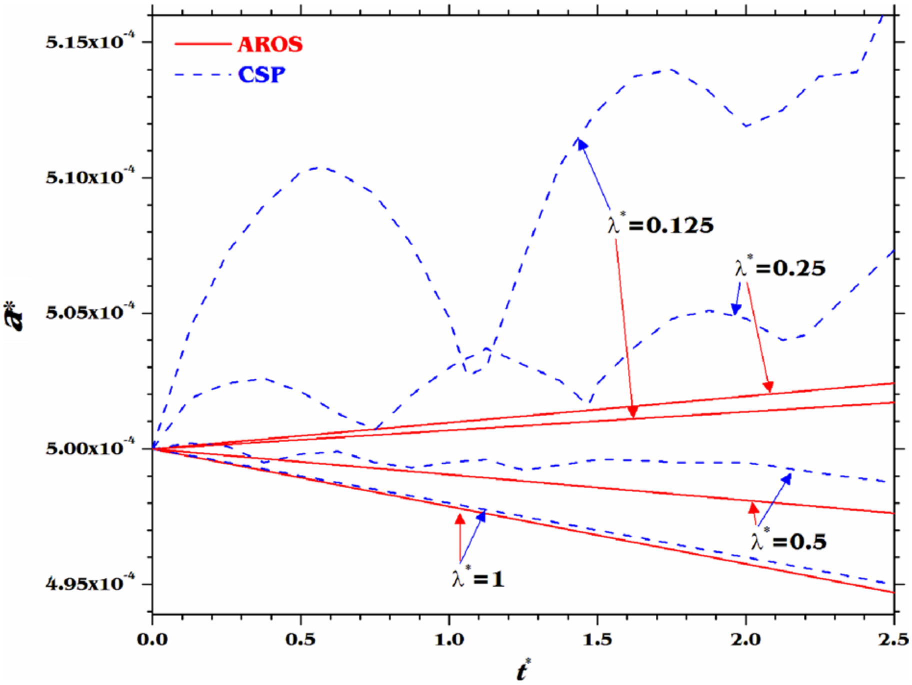

Fig. 4. Amplitude growth/decay curves for the several "unstable"/"stable" cases in Fig. 8a of CSP in comparison with AROS results. Note that in CSP even the two stable cases started out slightly unstable (their Fig. 8b).

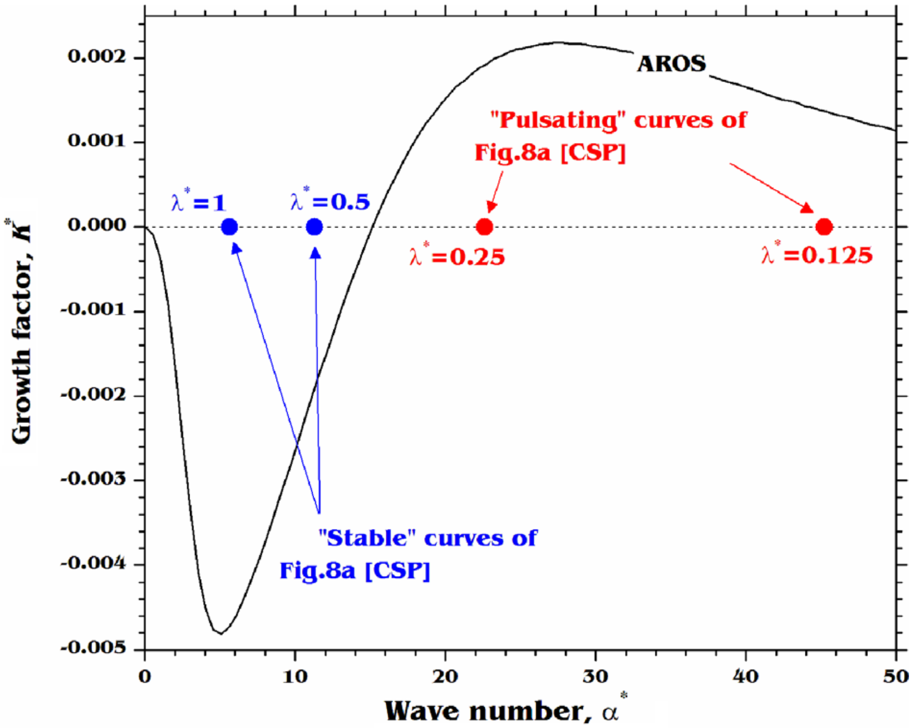

Fig. 5. The location of the four cases considered in Fig. 8 of CSP on the dispersion diagram determined by AROS.

Table 5
Illustration of the breakdown of the Long-wave theory as the "small parameter" condition $\alpha R < < 1$ is violated

Wavenumber, α	c_r (AROS)	c_i (AROS)	c_r (Long-wave)	c_i (Long-wave)
0.00001	0.8942417	−0.288369e−8	0.8942417	−0.288369e−8
.001	0.89424	−0.288369e−6	0.89424	−0.288369e−6
.01	0.89424	−0.288373e−5	0.89424	−0.288369e−5
.1	0.89423	−0.288740e−5	0.89424	−0.288369e−4
1	0.89299	−0.319908e−3	0.89424	−0.288369e−3
5.6554 ($\lambda^* = 1.0$)	0.89566	−0.750893e−3	0.89424	−0.163084e−2
11.3109 ($\lambda^* = 0.5$)	0.94875	−0.151780e−3	0.89424	−0.326171e−2
22.6217 ($\lambda^* = 0.25$)	0.99313	0.765712e−4	0.89424	−0.652340e−2
45.2435 ($\lambda^* = 0.125$)	0.99991	0.272234e−4	0.89424	−0.130468e−1

The CSP case considered is: $R = 0.47$, $m = 0.5$, $n = 0.11$, along with the last four wavelengths in the table. The values of αR are 2.65, 5.3, 10.6, and 21.2, respectively. Note that the errors are significant when $\alpha R > 0.1$, but it is interesting that the qualitative result (stable/unstable) is preserved (the first two cases) until there is an egregious violation of this condition (the last two cases).

Acknowledgements

This work was supported by the Joint Science and Technology Center of the Defense Threat Reduction Agency (JSTO/DTRA), and the National Ground Intelligence Center (NGIC). The support and collaboration of Mr. C. Fromer, J. Hanna, F. Handler, and R. Babarsky is gratefully acknowledged.

References

Boeck, T., Zaleski, S., 2005. Viscous versus inviscid instability of two-phase mixing layers with continuous velocity profile. Phys. Fluids 17, 032106.

Brackbill, J.U., Kothe, D.B., Zemac, C., 1992. A continuum method for modeling surface-tension. J. Comput. Phys. 100, 335–354.

Cao, Q., Sarkar, K., Prasad, A.K., 2004. Direct numerical simulations of two-layer viscosity-stratified flow. Int. J. Multiphase Flow 30, 1485–1508.

Coward, A.V., Renardy, Y.Y., Renardy, M., Richards, J.R., 1997. Temporal evolution of periodic disturbances in two-layer Couette flow. J. Comput. Phys. 132, 346–361.

Drazin, P.G., 1962. On stability of parallel flow of an incompressible fluid of variable density and viscosity. Proc. Cambridge Phil. Soc. 58, 646–661.

Griffith, B.E., Peskin, C.S., 2005. On the order of accuracy of the immersed boundary method: higher order rates for sufficiently smooth problems. J. Comput. Phys. 208, 75–105.

Hooper, A.P., Grimshaw, R., 1985. Nonlinear instability at the interface between 2 viscous fluids. Phys. Fluids 28, 37–45.

Khomami, B., Su, K.C., 2000. An experimental/theoretical investigation of interfacial instabilities in superposed pressure-driven channel flow of Newtonian and well characterized viscoelastic fluids. Part I: linear stability and encapsulation effects. J. Non-Newton. Fluid Mech. 91, 59–84.

Malik, S.V., Hooper, A.P., 2005. Linear stability and energy growth of viscosity stratified flows. Phys. Fluids 17, 024101.

Nourgaliev, R.R., Theofanous, T.G., 2006c. High-fidelity interface tracking in compressible flows: unlimited anchored adaptive level set. J. Comput. Phys. doi:10.1016/j.jcp.2006.10.031.

Nourgaliev, R.R., Dinh, T.N., Theofanous, T.G., 2006a. Adaptive characteristics-based matching for compressible multifluid dynamics. J. Comput. Phys. 213, 500–529.

Nourgaliev, R.R., Liou, M.S., Theofanous, T.G., 2006b. Numerical prediction of interfacial instability. In: The Fourth International Conference on Computational Fluid Dynamics, ICCFD'4, July 10–14, Ghent, Belgium.

Orszag, S., 1971. Accurate solution of the Orr–Sommerfeld stability equation. J. Fluid Mech. 50, 689.

Pinarbasi, A., Liakopoulos, A., 1995. The role of variable viscosity in the stability of channel flow. Int. Commun. Heat Mass Transfer 22, 837–847.

Su, Y.Y., Khomami, B., 1992. Numerical solution of eigenvalue problems using spectral techniques. J. Comput. Phys. 100, 297–305.

Theofanous, T.G., Nourgaliev, R., Khomami, B., in press. An experimental/theoretical investigation of interfacial instabilities in superposed pressure-driven channel flow of Newtonian and well characterized viscoelastic fluids. Part I: linear stability and encapsulation effects. J. Non-Newtonian Fluid Mech.

Unverdi, S.O., Tryggvason, G., 1992. A front-tracking method for viscous, incompressible, multi-fluid flows. J. Comput. Phys. 100, 25–37.

Yiantsios, S.G., Higgins, B.G., 1988. Linear stability of plane Poiseuille flow of two superposed fluids. Phys. Fluids 31, 3225.

Yih, C.S., 1967. Instability due to viscosity stratification. J. Fluid Mech. 27, 337.